Pergamon

Int. J. Heat Mass Transfer. Vol. 41, No. 16, pp. 2553–2555, 1998

Printed in Great Britain
0017–9310/98 $19.00+0.00

PII: S0017–9310(97)00246–9

Study of suspended vaporizing volatile liquid droplets by an enhanced sensitivity holographic technique: additional results

G. TOKER† and J. STRICKER

Faculty of Aerospace Engineering, Technion—Israel Institute of Technology, Haifa 32000, Israel

(*Received* 22 *August* 1997 *and in final form* 22 *September* 1997)

1. INTRODUCTION

Evaporation of a single isolated droplet in stagnant surrounding gas has been extensively studied both experimentally and theoretically, as reviewed in refs. [1–3].

In a previous paper [4] the dual hologram approach was suggested for direct measurements of the radial distribution of the change in the refractive index caused by the vapor molecules, Δn, in the vicinity of the vaporizing volatile liquid droplets as a function of time and droplet size. The reduction of interferometric data allowed the determination of saturation pressures, vapor densities and temperatures at the droplet surface of chloroform, acetone and diethyl ether. Due to the limited sensitivity of the measuring method, relatively large droplets, with diameters of the order of 2.5 mm were studied to increase the optical path in the air-vapor mixture. In addition, a stainless steel fiber with high thermal conductivity was used for suspending the droplets to enhance the heat transfer to the droplet and therefore to increase the vapor density.

In the present paper, a study of vaporizing volatile liquid droplets is performed, with diameters of the order of 1.5 mm, suspended from a tip of a plastic fiber of diameter 0.28 mm with low thermal conductivity characteristics. An attempt has been made to use small diameter droplets and low heat transfer through the suspending fiber, to extend the evaporation research to smaller diameter droplets with lower surface temperature. The droplet substances investigated are chloroform, acetone and diethyl ether [4], and, additionally, *n*-pentane. The limited sensitivity difficulty encountered in studying the vaporizing process of small droplets has been resolved by using a novel technique, known as the dual hologram interferometry with sensitivity enhancement. The technique provides a series of interferograms with remarkable fringe shifts even for such weak phase objects. The reduction of the interferometric data leads to the evaluation of the saturation pressures, the vapor densities and the temperatures at the droplet surfaces, and the radial variation the index of refraction, for all the four substances. By assuming a theoretical radial temperature profile, the radial variation of the vapor concentration can be obtained.

2. EXPERIMENTAL

A classic Mach–Zehnder interferometric scheme was used for recording low carrier frequency, 20–50 lines mm^{-1}, master holograms by the standard off-axis technique [4] on Agfa Copex Pan A.H.U. film. As a source of coherent radiation, a continuous wave argon ion laser operating at wavelength, $\lambda = 514.5$ nm, was used. The dynamics of vaporization was investigated by holographing the droplet on the film with a minimal time interval between frames of 6 s.

† Author to whom correspondence should be addressed.

2.1. *Dual hologram interferometry with sensitivity enhancement*

The conventional dual hologram technique enables us to reliably measure a fringe shift of the order of 1/10 of the fringe. For a vaporizing acetone droplet, with a maximum typical optical path length of the order of $\lambda/4$, this means an accuracy of the order of 40%. It becomes apparent that, to obtain the adequate accuracy for such weak phase objects, phase detection methodology must provide very accurate measurements, of the order of $\lambda/40$ or even lower.

In order to increase the sensitivity of the conventional interference analysis, we successfully applied the dual hologram enhanced sensitivity method [5]. This method is based on the properties of a non-linearly recorded hologram and is accomplished by the technique for re-recording holograms [6] to increase the wave front deformation in the higher diffraction orders. It follows from the analysis in ref. [6] that the phase difference in the m-th diffraction order is increased m times the actual shift caused by the vapor. The droplet and the no-droplet re-recorded holograms, obtained by using the ± 2nd orders of the master holograms, were spatially superposed and illuminated by the reconstructing wave. The intensity distribution in the resulting interference pattern has the form:

$$I \sim 1+\cos[(4\Delta\varepsilon(x,y)], \tag{1}$$

where $\Delta\varepsilon(x,y)$ is the actual phase change caused by the vapor. Expression (1) describes an interferogram with sensitivity increased by a factor of four and with compensation for the aberrations of the optical systems for recording and re-recording holograms. The aberration-free feature of this method is the principle for the study of the weakly-refracting air-vapor mixtures.

Typical finite width fringes interferograms obtained with the conventional dual hologram technique (a) and with the enhanced sensitivity method (b), for a *n*-pentane droplet, are shown in Fig. 1. The sensitivity of the reconstructed interferogram in Fig. 1(b) is increased by a factor of four. It should be emphasized that to obtain the reconstructed interferograms, shown in Fig. 1(a) and (b), the same master droplet and no-droplet holograms were used.

2.2. *Determination of molecular vapor density, partial vapor pressure and temperature on the droplet surface*

The phase enhancement technique made it possible to obtain reconstructed interferograms with remarkable fringe shifts [see Fig. 1(b)] and to reliably calculate the radial density distribution of the refractive index around small cold droplets. The process of interferometric data reduction and determination of radial distribution of $\Delta n(r) = n(r) - n_\infty$, where n_∞ is the index of refraction of the undisturbed air at room temperature and pressure, was described in detail in [4]. Such radial distributions of Δn were calculated for the equatorial cross-sections only. The obtained radial distribution of $\Delta n(r)$ in the vicinity of the droplet surface permits the deter-

NOMENCLATURE

a	droplet radius
b	boundary of free convection
C_v	coefficient of refractivity of separate vapor molecule $C_v = (n_v^0 - 1)/N_0$
C_g	coefficient of refractivity of separate air molecule
I	intensity of light in interforometric pattern
m	diffraction order
n	refractive index
n_v^0	refractive index of vapor at normal conditions
N_v	vapor molecular density
N_0	Loschmidt number [2.687×10^{19} cm^{-3}]
N_∞	surrounding air molecular density [2.504×10^{19} cm^{-3}]
P_v	partial vapor pressure
P_0	normal pressure [760 mm Hg]
P_∞	surrounding air pressure [760 mm Hg]
r	radius
T	temperature
T	normal temperature [273 K]
T_∞	surrounding air temperature [293 K]
x, y, z	coordinates.

Greek symbols

Δ	change of parameter
λ	wavelength of diagnostic beam
ξ	dimentionless variable, r/a
σ	actual phase of the object light wave.

Subscripts

a	at the droplet surface
g	gas phase (air)
s	saturated
v	vapor
va	vapor parameters at the droplet surface
0	normal conditions
∞	surrounding air conditions.

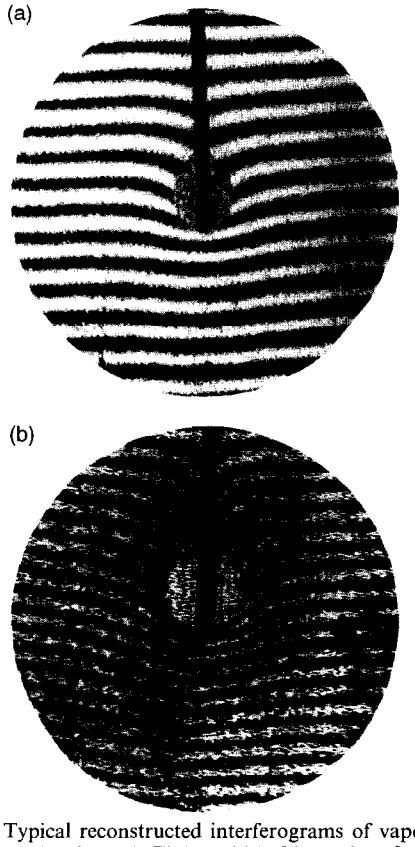

Fig. 1. Typical reconstructed interferograms of vaporizing n-pentane droplet. (a) Finite width fringes interferogram obtained by dual hologram technique; (b) finite width fringes interferogram obtained by dual hologram with enhanced sensitivity method. Sensitivity was increased by a factor of 4.

mination of the coefficients of refraction, $(\Delta n)_a$, on the droplet surface. As was discussed in [4], the value, $(\Delta n)_a$, can be used to evaluate the molecular vapor density, N_{va}, saturation pressure, P_{va}, and temperature, T_a, on the droplet surface by using the expression:

$$\frac{N_v}{N_\infty} = \frac{\Delta n}{N_\infty (C_v - C_g)} - \frac{C_g}{(C_v - C_g)}\left(\frac{T_\infty}{T} - 1\right), \qquad (2)$$

where T is the temperature of the air–vapor mixture at the point (x, y, z), T_∞ is the temperature of the undisturbed surrounding air, C_g and C_v are the coefficients of refractivity for air and a vapor molecule, respectively. C is defined as $C = (n^0 - 1)/N_0$, where n^0 is the index of refraction at normal conditions, and N_0 is the Loschmidt number. The pressures P_{va}, the vapor molecular densities N_{va} and the surface temperatures T_a thus obtained are given in Table 1.

2.3. *Effect of free convection on the radial distribution of vapor density*

The reduction of interference data confirmed the fact [4] that in nominally still air, free convection takes place. The air movement abruptly reduces the vapor concentration far from the droplet surface at a radial distance denoted by b. It was found that b is independent of droplet size. The values b, are shown in Table 1.

Equation (2) indicates that temperature and concentration of the vapor can be determined separately only on the droplet surface. In order to obtain the concentration profiles far from the droplet surface, a theoretical temperature profile was used, given by [3]:

$$\frac{T}{T_\infty} = \frac{T_a}{T_\infty} + \frac{b}{r}\frac{r-a}{b-a}\left(1 - \frac{T_a}{T_\infty}\right) \quad \text{for } a \leqslant r \leqslant b \qquad (3)$$

Equation (3) was developed for a spherical low volatile liquid droplet, located at the center of a spherical enclosure. The enclosure radius is b and its wall temperature is T_∞. It was assumed that the profile described by equation (3) is true also for a volatile droplet suspended in unbounded still air (see also ref. [4]). For this case, the enclosure radius b is replaced by the boundary of free convection, and the wall temperature by T_∞, the temperature of the undisturbed surrounding air. Figures 2 and 3 show the vapor molecular density variation obtained from equations (2) and (3) for the four substances. The radial distance, $\xi_b = b/a$, at which the abrupt reduction of N_v occurs, is marked in the figures.

3. SUMMARY AND RESULTS

For the first time the dual hologram approach with enhanced sensitivity was applied to study the dynamics of

Table 1. Parameters characterizing vaporization of suspended volatile liquid droplets in still air at $T_\infty = 293$ K, $P_\infty = 760$ mm Hg

Substance	T (K)	P_{va} (mm Hg)	N_{va} (10^{-18} cm^{-3})	b (mm)
Chloroform	269±2	48±4	1.7±0.12	1.7±0.1
Acetone	249±2	15±2	0.6±0.10	2.7±0.1
Diethyl ether	244±2	37±4	1.5±0.12	2.0±0.1
n-Pentane	245±2	43±4	1.7±0.12	2.0±0.1

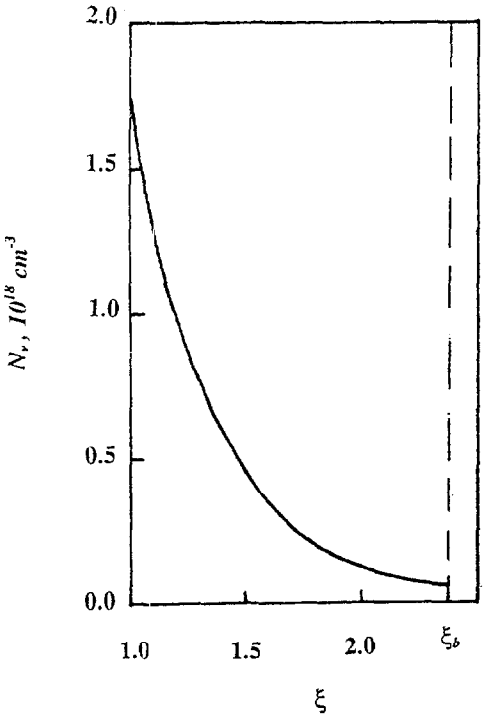

Fig. 2. Radial distribution of vapor density vs dimensionless variable $\xi = r/a$. Chloroform droplet. Droplet radius $a = 720$ μm.

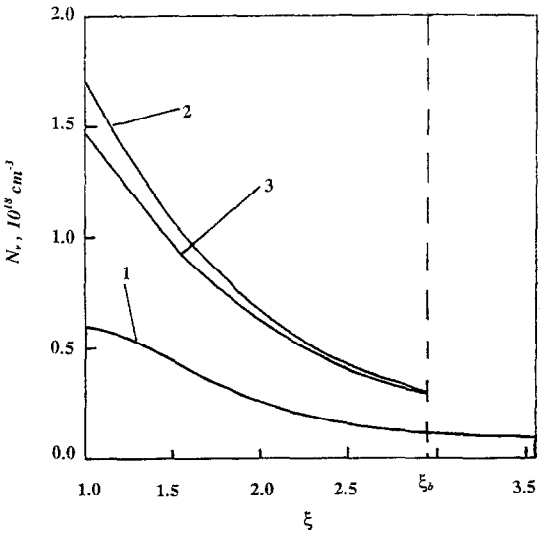

Fig. 3. Radial distribution of vapor density vs dimensionless variable $\xi = r/a$. (1) Acetone droplet. Droplet radius $a = 760$ μm. (2) *n*-Pentane droplet. Droplet radius $a = 680$ μm. (3) Diethyl ether droplet. Droplet radius $a = 680$ μm.

vaporization of suspended single droplets in unbounded still air. The method made it possible to study smaller size droplets with lower surface temperatures as compared to those studied in ref. [4].

(a) The three main results obtained in ref. [4] were confirmed in the present study:

(1) The change of the refractive index $(\Delta n)_a$, at the surface of a vaporizing volatile droplet does not depend on the droplet size as long as the droplet is large enough in comparison with the suspending fiber. Δn decreases exponentially with similar dimensionless variable $\xi = r/a$.

(2) Free convection effects are important at $r > b$, where an abrupt decrease in vapor concentration occurs. The temperature T_a is weakly affected by free convection effects.

(3) Based on the assumption that the actual temperature is close to a spherically symmetric distribution of a low volatile droplet, described by Equation (3), the radial vapor density distribution was calculated for the droplets of all the four substances.

(b) At conditions where intensive heat transfer through the suspending fiber was removed, the surface temperatures become lower by 5–8 K as compared to those in [4]. Accordingly, the vapor pressure at the droplet surface decreased by 24, 42 and 37% for chloroform, acetone and diethyl ether, respectively.

(c) *n*-Pentane was studied in addition to the substances investigated in [4]. It was observed that *n*-pentane droplets vaporization dynamics are similar to diethyl ether (see Table 1 and Fig. 3).

REFERENCES

1. Faeth, G. M., Current status of droplet and liquid combustion. *Prog. Energy Combustion Sci.*, 1977, **3**, 191–224.
2. Sirignano, W. A., Fuel droplet vaporization and spray combustion. *Prog. Energy Combustion Sci.*, 1983, **9**, 291–322.
3. Fuchs, N. A., *Evaporation and Droplet Growth in Gaseous Media*. Pergamon Press, Oxford, 1959.
4. Toker, G. R. and Stricker, J., Holographic study of suspended vaporizing volatile liquid droplets in still air. *Int. J. Heat Mass Trans.*, 1996, **39**, 3475–3482.
5. Zeilikovich, I., Lyalikov, A. and Toker, G., Visualization of acoustic waves in a dye solution by holographic interferometry. *Sov. Tech. Phys. Letts*, 1988, **14**, 213–214.
6. Zeilikovich, I. S. and Lyalikov, A. M., Holographic methods for regulating the sensitivity of interference measurements for transparent media diagnostics. *Sov. Physics USPEKHI*, 1991, **34**, 74–85.